Annals of Physics 324 (2009) 1783–1795

Contents lists available at ScienceDirect

Annals of Physics

journal homepage: www.elsevier.com/locate/aop

Efficient weakly-radiative wireless energy transfer: An EIT-like approach

Rafif E. Hamam *, Aristeidis Karalis, J.D. Joannopoulos, Marin Soljačić

Center for Materials Science and Engineering and Research Laboratory of Electronics, Massachusetts Institute of Technology, Cambridge, MA 02139, USA

ARTICLE INFO

Article history:
Received 5 December 2008
Accepted 15 May 2009
Available online 27 May 2009

Keywords:
Wireless energy transfer
Coupling
Electromagnetically induced transparency (EIT)
Stimulated Raman Adiabatic Passage (STIRAP)
Adiabatic following
Coupled mode theory
Resonance

ABSTRACT

Inspired by a quantum interference phenomenon known in the atomic physics community as electromagnetically induced transparency (EIT), we propose an efficient weakly radiative wireless energy transfer scheme between two identical classical resonant objects, strongly coupled to an intermediate classical resonant object of substantially different properties, but with the same resonance frequency. The transfer mechanism essentially makes use of the adiabatic evolution of an instantaneous (so called "dark") eigenstate of the coupled 3-object system. Our analysis is based on temporal coupled mode theory (CMT), and is general enough to be valid for various possible sorts of coupling, including the resonant inductive coupling on which witricity-type wireless energy transfer is based. We show that in certain parameter regimes of interest, this scheme can be more efficient, and/or less radiative than other, more conventional approaches. A concrete example of wireless energy transfer between capacitively-loaded metallic loops is illustrated at the beginning, as a motivation for the more general case. We also explore the performance of the currently proposed EIT-like scheme, in terms of improving efficiency and reducing radiation, as the relevant parameters of the system are varied.

1. Introduction

The decade has witnessed a considerable interest in energy issues, such as safe generation of renewable energy, energy storage and management, etc. In particular, there is a substantial recent interest [1–5] in enabling efficient and safe wireless energy transfer, motivated by the increased

* Corresponding author.
E-mail address: rafif@mit.edu (R.E. Hamam).

0003-4916/$ - see front matter © 2009 Elsevier Inc. All rights reserved.
doi:10.1016/j.aop.2009.05.005

involvement of autonomous electronic devices (e.g. laptops, cell phones, household robots) in almost all aspects of our everyday lives, and the need to charge those devices repeatedly. In this respect, wireless nonradiative energy transfer schemes have been recently proposed [6,7] based on strong coupling between electromagnetic resonances. In this work, we explore a somewhat different scheme of efficient energy transfer between resonant objects coupled in some general way. Instead of transferring energy directly between the two resonant objects, an intermediate resonant object will be used to mediate the transfer. The intermediate object is chosen such as to couple very strongly to each of the objects involved in the energy transfer (i.e. much more strongly than the other two objects couple to each other). In practice, enabling such strong coupling will usually come with a price; in typical situations, the mediating object will often be substantially radiative. Yet, surprisingly enough, the proposed "indirect" energy transfer scheme will be shown to be efficient and weakly-radiative by merely introducing a meticulously chosen time variation of the coupling rates. The inspiration as to why the particular time variation had to work so well comes from a quantum interference phenomenon, known in the atomic physics community as electromagnetically induced transparency [8] (EIT). In EIT, 3 atomic states participate. Two of them (which are non-lossy) are coupled to one that has substantial losses. However, by meticulously controlling the mutual couplings between the states, one can establish a coupled system which is overall non-lossy. This manifests itself in that a medium that is originally highly opaque to some laser pulse (called "probe" laser), can be made transparent by sending through it another laser pulse (called "Stokes" laser), provided that the temporal overlap between the two pulses is properly chosen. A closely related phenomenon known as Stimulated Raman Adiabatic Passage (STIRAP) [9–11] takes place in a similar system; namely, the probe and Stokes laser can be used to achieve a complete coherent population transfer between two molecular states of the medium. Hence, we refer to the currently proposed scheme as the "EIT-like" energy transfer scheme.

To set the stage for our proposed indirect energy transfer scheme, we will first consider (in Section 2) one concrete example of wireless energy transfer between two resonant capacitively-loaded conducting-wire loops [6], and show how the indirect EIT-like scheme can be made more efficient and less-radiative in this particular system than the direct scheme, by including proper time variations in the coupling rates. In Section 3, we analyze the underlying physical mechanism which turns out to be applicable not just to "wireless" energy transfer, but more generally to any sort of energy transfer between resonant objects. The analysis will be based on temporal coupled mode theory (CMT) [12], which is a valid description for well-defined resonances with large quality factors. In Section 4, we study the general case of EIT-like energy transfer, how the transferred and lost energies vary with the rates of coupling and loss, both with and without time variation of the coupling rates; we also investigate the range of relevant parameters in which the radiated energy is substantially reduced by using the EIT-like scheme.

2. An illustrative example of an EIT-like system

We start with a concrete case of wireless energy transfer between two identical resonant conducting loops, labeled by L_1 and L_3. The loops are capacitively-loaded and couple inductively via their mutual inductance. Let r_A denote the loops' radii, N_A their numbers of turns, and b_A the radii of the wires making the loops. We also denote by D_{13} the center-to-center separation between the loops. Resonant objects of this type have two main loss mechanisms: ohmic absorption, and far-field radiation. Using the same theoretical method from Ref. [6], we find that for $r_A = 7$ cm, $b_A = 6$ mm, and $N_A = 15$ turns, the quality factors for absorption and radiation are, respectively, $Q_{abs}^{(A)} \equiv 2\pi f/\Gamma_{abs}^{(A)} = 3.19 \times 10^4$ and $Q_{rad}^{(A)} \equiv 2\pi f/\Gamma_{rad}^{(A)} = 2.6 \times 10^5$ at a resonant frequency $f = 1.8 \times 10^7$ Hz (remember that L_1 and L_3 are identical and have the same properties). $\Gamma_{abs}^{(A)}$, $\Gamma_{rad}^{(A)}$ are, respectively, the rates of absorptive and radiative loss of L_1 and L_3, and the rate of coupling between L_1 and L_3 is denoted by κ_{13}. When the loops are in fixed distinct parallel planes separated by $D_{13} = 1.4$ m and have their centers on an axis (C) perpendicular to their planes, as shown in Fig. 1a, the quality factor for inductive coupling is $Q_\kappa \equiv 2\pi f/\kappa_{13} = 1.3 \times 10^4$, independent of time. This configuration of parallel loops corresponds to the largest possible coupling rate κ_{13} at the particular separation D_{13}. We denote the amplitude of the electric field of the resonant mode of L_1 by a_1, and that of L_3 by a_3. As long as all the quality factors involved are large enough, the time evolution of the mode amplitudes a_1 and a_3 can be modeled according to the following temporal CMT equations [12]:

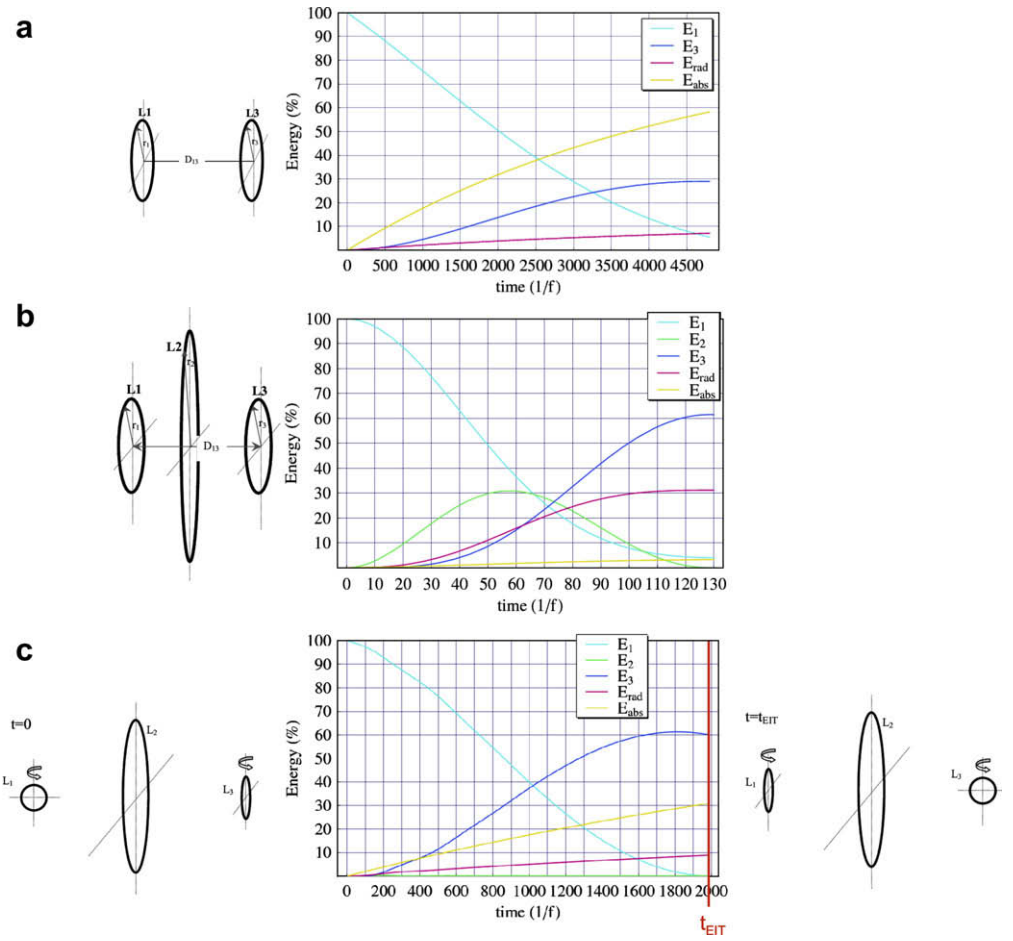

Fig. 1. Wireless energy transfer in an examplary system: (a) (left) Schematic of loops configuration in 2-object direct transfer. (Right) Time evolution of energies in the 2-object direct energy transfer case. (b) (left) Schematic of 3-loops configuration in the constant-κ case. (right) Dynamics of energy transfer for the configuration in (b, left). Note that the total energy transferred E_3 is two times larger than in (a, right), but at the price of the total energy radiated being four times larger. (c) (left) Loop configuration at $t = 0$ in the EIT-like scheme. (Center) Dynamics of energy transfer with EIT-like rotating loops. (Right) Loop configuration at $t = t_{EIT}$. Note that E_3 is comparable to (b, right), but the radiated energy is now much smaller: in fact, it is comparable to (a, right).

$$\frac{da_1}{dt} = -(i\omega + \Gamma_A)\, a_1 + i\kappa_{13} a_3 \tag{1}$$

$$\frac{da_3}{dt} = -(i\omega + \Gamma_A)\, a_3 + i\kappa_{13} a_1 \tag{2}$$

where $\omega = 2\pi f$ is the angular resonance frequency, and $\Gamma_A = \Gamma_{rad}^{(A)} + \Gamma_{abs}^{(A)}$. The mode amplitudes $a_1(t)$ and $a_3(t)$ are normalized such that $|a_1(t)|^2$ and $|a_3(t)|^2$ represent, respectively, the energies in L_1 and L_3 at time t: $E_1(t) \equiv |a_1(t)|^2$ and $E_3(t) \equiv |a_3(t)|^2$. Starting with 100% of the total energy being initially in L_1 (i.e. $|a_3(t=0)|^2 = 0$), we find that the energy transferred to L_3 is maximum at time $t_a = 4774.6(1/f)$, and constitutes 29% of the initial total energy, as shown in Fig. 1a. The energies radiated $E_{rad}(t_a)$ and absorbed $E_{abs}(t_a)$ up to time t_a constitute, respectively, 7.2% and 58.1% of the initial total energy, with 5.8% of the energy remaining in L_1. The CMT expressions used for $E_{rad}(t_a)$ and $E_{abs}(t_a)$ are given by:

$$E_{rad}(t_a) = \int_0^{t_a} \left(2\,\Gamma_{rad}^{(A)}|a_1(t)|^2 + 2\Gamma_{rad}^{(A)}|a_3(t)|^2\right)dt \tag{3}$$

$$E_{abs}(t_a) = \int_0^{t_a} \left(2\Gamma_{abs}^{(A)}|a_1(t)|^2 + 2\Gamma_{abs}^{(A)}|a_3(t)|^2\right)dt \tag{4}$$

In order to improve the efficiency of the energy transfer from the current $\simeq$30%, we now consider different ways to boost the energy transferred from L_1 to L_3 while keeping the distance D_{13} separating them fixed. Since the relative orientations of the two loops are already chosen to yield the maximum κ_{13}, we no longer have much flexibility in improving the efficiency of transfer between these given resonant objects at the same separation D_{13}. So, we introduce an intermediate resonant object that couples strongly to both L_1 and L_3, while having the same resonant frequency as both of them. For the sake of illustration in the particular concrete system under consideration, we also take that mediator to be a capacitively-loaded conducting-wire loop, and we label it by L_2. We place L_2 at equal distance ($D_{12} = D_{23} = D_{13}/2 = 0.7$ m) from L_1 and L_3 such that its axis also lies on the same axis (C), and we orient it such that its plane is parallel to the planes of L_1 and L_3. In order for L_2 to couple strongly to L_1 and L_3, its size needs to be substantially larger than the size of L_1 and L_3. However this increase in the size of L_2 has a considerable drawback in the sense that it is also accompanied by a significant increase in the undesired radiated energy. This feature is quite generic for the resonant systems of this type: stronger coupling can often be enabled by increasing the objects' size, but it implies stronger radiation from the object in question. Large radiation is often undesirable because it could lead to far-field interference with other RF systems, and in some systems also because of safety concerns. For $r_B = 70$ cm, $b_B = 1.5$ cm, and $N_B = 1$ turn, we get $Q_{abs}^{(B)} \equiv 2\pi f/\Gamma_{abs}^{(B)} = 7706$, $Q_{rad}^{(B)} \equiv 2\pi f/\Gamma_{rad}^{(B)} = 400$, and $Q_{\kappa_{12}} \equiv 2\pi f/\kappa_{12} = Q_{\kappa_{23}} = 180$ at $f = 1.8 \times 10^7$ Hz. A schematic diagram of the 3-loops configuration is depicted in Fig. 1b. If we denote the amplitude of the E-field of the resonance mode in L_2 by a_2, then the CMT equations can be written as:

$$\frac{da_1}{dt} = -(i\omega + \Gamma_A)a_1 + i\kappa_{12}a_2 \tag{5}$$

$$\frac{da_2}{dt} = -(i\omega + \Gamma_B)a_2 + i\kappa_{12}a_1 + i\kappa_{23}a_3 \tag{6}$$

$$\frac{da_3}{dt} = -(i\omega + \Gamma_A)a_3 + i\kappa_{23}a_2 \tag{7}$$

Note that since the coupling rates κ_{12} and κ_{23} are $\simeq$70 times larger than κ_{13}, we can ignore the direct coupling between L_1 and L_3, and focus only on the indirect energy transfer through the intermediate loop L_2. If initially all the energy is placed in L_1, i.e. if $E_2(t=0) \equiv |a_2(t=0)|^2 = 0$ and $E_3(t=0) \equiv |a_3(t=0)|^2 = 0$, then the optimum in energy transferred to L_3 occurs at a time $t_b = 129.2(1/f)$, and is equal to $E_3(t_b) = 61.50\%$. The energy radiated up to t_b is $E_{rad}(t_b) = 31.1\%$, while the energy absorbed is $E_{abs}(t_b) = 3.3\%$, and 4.1% of the initial energy is left in L_1. Thus while the energy transferred, now indirectly, from L_1 to L_3 has increased by a factor of 2 relative to the 2-loops direct transfer case, the energy radiated has undesirably increased by a significant factor of 4. Also note that the transfer time in the 3-loops case is now $\simeq$35 times shorter than in the 2-loops direct transfer because of the stronger coupling rate. The dynamics of the energy transfer in the 3-loops case is shown in Fig. 1b, where the expressions used for $E_{rad}(t_b)$ and $E_{abs}(t_b)$ are given by:

$$E_{rad}(t_b) = \int_0^{t_b} \left(2\Gamma_{rad}^{A}|a_1(t)|^2 + 2\Gamma_{rad}^{B}|a_2(t)|^2 + 2\Gamma_{rad}^{A}|a_3(t)|^2\right)dt \tag{8}$$

$$E_{abs}(t_b) = \int_0^{t_b} \left(2\Gamma_{abs}^{A}|a_1(t)|^2 + 2\Gamma_{abs}^{B}|a_2(t)|^2 + 2\Gamma_{abs}^{A}|a_3(t)|^2\right)dt \tag{9}$$

Thus the switch from 2-loops direct transfer to 3-loops indirect transfer had an expected significant improvement in efficiency, but it came with the undesirable effect of increased radiated energy. Let us now consider some modifications to the 3-loops indirect transfer scheme, aiming to reduce the total radiated energy back to its reasonable value in the 2-loops direct transfer case, while maintaining the total energy transfer at a level comparable to Fig. 1b. As shown in Fig. 1c, we will keep the orientation of L_2 fixed, and start initially (t=0) with L_1 perpendicular to L_2 and L_3 parallel to L_2, then uniformly ro-

tate L_1 and L_3, at the same rates, until finally, at $(t = t_{EIT})$, L_1 becomes parallel to L_2 and L_3 perpendicular to it, where we stop the transfer process. This process can be modeled by the following time variation in the coupling rates:

$$\kappa_{12}(t) = \kappa \sin(\pi t/2t_{EIT}) \tag{10}$$

$$\kappa_{23}(t) = \kappa \cos(\pi t/2t_{EIT}) \tag{11}$$

for $0 < t < t_{EIT}$, and $Q_\kappa = 180.1$ as before. By using the same CMT analysis as in Eqs. (5)–(7), we find, in Fig. 1c, that for $t_{EIT} = 1989.4(1/f)$, an optimum transfer of 61.2% can be achieved at $t_c = 1,798.5(1/f)$, with only 8.2% of the initial energy being radiated, 28.6% absorbed, and 2% left in L_1. This is quite remarkable: by simply rotating the loops during the transfer, the energy radiated has dropped by a factor of 4, while keeping the same 61% level of the energy transferred, although the instantaneous coupling rates are now smaller than κ. This considerable decrease in radiation is on first sight quite counterintuitive, because the intermediate resonator L_2, which mediates all the energy transfer, is highly radiative ($\simeq$650 times more radiative than L_1 and L_3), and there is much more time to radiate, since the whole process lasts 14 times longer than in Fig. 1b.

A clue to the physical mechanism behind this surprising result can be obtained by observing the differences between the green curves in Fig. 1b and c. Unlike the case of constant coupling rates, depicted in Fig. 1b, where the amount of energy ultimately transferred to L_3 goes first through the intermediate loop L_2, in the case of time-varying coupling rates, shown in Fig. 1c, there is almost little or no energy in L_2 at all times during the transfer. In other words, the energy is transferred quite efficiently from L_1 to L_3, mediated by L_2 without ever being in the highly radiative intermediate loop L_2. (Note that direct transfer from L_1 to L_3 is identically zero here since L_1 is always perpendicular to L_3, so all the energy transfer is indeed mediated through L_2.) This surprising phenomenon is actually quite similar to the well-known electromagnetically induced transparency [8] (EIT), which enables complete population transfer between two quantum states through a third lossy state, coupled to each of the other two states.

3. Physical mechanism behind EIT-like energy transfer scheme

We note that the mechanism explored in the previous section is not restricted to wireless energy transfer between inductively coupled loops, but its scope extends beyond, to the general case of energy transfer between resonant objects (henceforth denoted by R_i) coupled in some general way. So, all the rest of this article falls in this general context, and the only constraints for the EIT-like scheme are that the three resonant objects have the same resonance angular frequency, which we denote by ω_o, that all quality factors be large enough for CMT to be valid, and that the initial and final resonant objects have the same loss rate Γ_A. R_1 and R_3 will be assumed to have negligible mutual interactions with each other, while each of them can be strongly coupled to R_2. However, as is often the case in practice of wireless power transfer [6], R_2's strong coupling with other objects will be assumed to be accompanied with its inferior loss properties compared to R_1 and R_3, usually in terms of substantially larger radiation losses. To analyze the problem in detail, we start by rewriting the CMT Eqs. (5)–(7) in matrix form, and then diagonalizing the resulting time evolution operator $\widehat{C}(t)$.

$$\frac{d}{dt}\begin{pmatrix} a_1 \\ a_2 \\ a_3 \end{pmatrix} = \begin{pmatrix} -(i\omega_o + \Gamma_A) & i\kappa_{12} & 0 \\ i\kappa_{12} & -(i\omega_o + \Gamma_B) & i\kappa_{23} \\ 0 & i\kappa_{23} & -(i\omega_o + \Gamma_A) \end{pmatrix}\begin{pmatrix} a_1 \\ a_2 \\ a_3 \end{pmatrix} \equiv \widehat{C}(t)\begin{pmatrix} a_1 \\ a_2 \\ a_3 \end{pmatrix} \tag{12}$$

In the special case where the coupling rates κ_{12} and κ_{23} are constant and equal, Eq. (12) admits a simple analytical solution, presented in the appendix. In the more general case of time dependent and unequal coupling rates $\kappa_{12}(t)$ and $\kappa_{23}(t)$, the CMT operator $\widehat{C}(t)$ has an interesting feature which results from the fact that one of its eigenstates, $\vec{V}_1$, with complex eigenvalue $\lambda_1 = -(i\omega_o + \Gamma_A)$, has the form

$$\vec{V}_1 = e^{-i\omega_o t - \Gamma_A t}\begin{pmatrix} \frac{-\kappa_{23}}{\sqrt{(\kappa_{12})^2 + (\kappa_{23})^2}} \\ 0 \\ \frac{\kappa_{12}}{\sqrt{(\kappa_{12})^2 + (\kappa_{23})^2}} \end{pmatrix} \tag{13}$$

This eigenstate $\vec{V}_1$ is the most essential building block of our proposed efficient weakly-radiative energy transfer scheme, because it has no energy at all in the intermediate (lossy) resonator R_2, i.e. $a_2(t) = 0 \,\forall\, t$ whenever the 3-object system is in state $\vec{V}_1$. In fact if $\Gamma_A \to 0$, then the EIT-like energy transfer scheme can be made completely nonradiative, no matter how large is the radiative rate Γ^B_{rad}, as shown in Fig. 2. Moreover, if the 3-object system is in state $\vec{V}_1$, then $\kappa_{12} = 0$ corresponds to all the system's energy being in R_1, while $\kappa_{23} = 0$ corresponds to all the system's energy being in R_3. So, the important considerations necessary to achieve efficient weakly radiative energy transfer, consist of preparing the system initially in state $\vec{V}_1$. Thus, if at $t = 0$ all the energy is in R_1, then one should have $\kappa_{12}(t = 0) = 0$ and $\kappa_{23}(t = 0) \neq 0$. In the loops' case where coupling is performed through induction, these values for κ_{12} and κ_{23} correspond to exactly the same configuration that we had considered in Fig. 1c, namely starting with $L_1 \perp L_2$ and $L_3 \parallel L_2$. In order for the total energy of the system to end up in R_3, we should have $\kappa_{12}(t = t_{EIT}) \neq 0$ and $\kappa_{23}(t = t_{EIT}) = 0$. This ensures that the initial and final states of the 3-object system are parallel to $\vec{V}_1$. However, a second important consideration is to keep the 3-object system at all times in $\vec{V}_1(t)$, even as $\kappa_{12}(t)$ and $\kappa_{23}(t)$ are varied in time. This is crucial in order to prevent the system's energy from getting into the intermediate object R_2, which may be highly radiative as in the example of Fig. 1, and requires changing $\kappa_{12}(t)$ and $\kappa_{23}(t)$ slowly enough so as to make the entire 3-object system adiabatically follow the time evolution of $\vec{V}_1(t)$. The criterion for adiabatic following can be expressed, in analogy to the population transfer case[9], as

$$\left| \left\langle \vec{V}_{2,3} \middle| \frac{d\vec{V}_1}{dt} \right\rangle \right| \ll \left| \lambda_{2,3} - \lambda_1 \right| \tag{14}$$

where $\vec{V}_2$ and $\vec{V}_3$ are the remaining two eigenstates of $\widehat{C}(t)$, with corresponding eigenvalues λ_2 and λ_3. In principle, one would think of making the transfer time t_{EIT} as long as possible to ensure adiabaticity. However there is a limitation on how slow the transfer process can optimally be, imposed by the losses in R_1 and R_3. Such a limitation may not be a strong concern in a typical atomic EIT case, because the initial and final states there can be chosen to be non-lossy ground states. However, in our case, losses in R_1 and R_3 are not avoidable, and can be detrimental to the energy transfer process whenever the transfer time t_{EIT} is not less than $1/\Gamma_A$. This is because, even if the 3-object system is carefully kept in $\vec{V}_1$ at all times, the total energy of the system will decrease from its initial value as a consequence of losses in R_1 and R_3. Thus the duration of the transfer should be a compromise between these two limits: the desire to keep t_{EIT} long enough to ensure near-adiabaticity, but short enough not to suffer from losses in R_1 and R_3.

We can now also see in the EIT framework why is it that we got a considerable amount of radiated energy when the inductive coupling rates of the loops were kept constant in time, i.e. in constant-κ case, like in Fig. 1b. The reason is that, when $\kappa_{12} = \kappa_{23} =$const, the energies in R_1 and R_3 will always be equal to each other if the 3-object system is to stay in $\vec{V}_1$. So one cannot transfer energy from R_1 to R_3 by keeping the system purely in state $\vec{V}_1$; note that even the initial state of the system, in which all

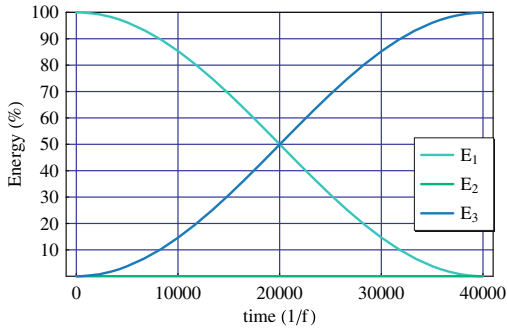

Fig. 2. Energy transfer with time-varying coupling rates, for $\Gamma_A = 0$, $\kappa/\Gamma_B = 10, \kappa_{12} = \kappa \sin(\pi t/(2t_{EIT}))$, and $\kappa_{23} = \kappa \cos(\pi t/(2t_{EIT}))$.

the energy is in R_1, is not in $\vec{V}_1$, and has nonzero components along the eigenstates $\vec{V}_2$ and $\vec{V}_3$ which implies a finite energy in R_2, and consequently result in an increased radiation, especially if $\Gamma^B_{rad} \gg \Gamma^A_{rad}$ as in our concrete example.

Although the analysis presented above, in terms of the adiabatic following of the eigenstate $\vec{V}_1$, clarifies why the EIT-like transfer scheme is weakly radiative, this explanation still seems to be puzzling and somewhat paradoxical. The origin of the paradox stems from the fact that, in the EIT-like approach, there is no energy at all in the mediator R_2. That is to say, energy is efficiently transferred through the intermediate resonator R_2 without ever being in it. This apparent contradiction can be resolved by looking at the detailed contributions to the time-rate of change of the energy E_2 in R_2. As we show it in more details in the appendix, the EIT-like approach ensures that the energy leaves R_2 (to R_3) as soon as it reaches R_2 (from R_1).

4. Under which conditions is EIT-like approach beneficial?

In the abstract case of energy transfer from R_1 to R_3, where no constraints are imposed on the relative magnitude of κ, Γ^A_{rad}, Γ^B_{rad}, Γ^A_{abs} and Γ^B_{abs}, there is no reason to think that the EIT-like transfer is always better than the constant-κ one, in terms of the transferred and radiated energies. In fact, there could exist some range of the parameters (κ, Γ^A_{rad}, Γ^B_{rad}, Γ^A_{abs}, Γ^B_{abs}), for which the energy radiated in the constant-κ transfer case is less than that radiated in the EIT-like case. For this reason, we investigate both the EIT-like and constant-κ transfer schemes, as we vary all the crucial parameters of the system. The percentage of energies transferred and lost (radiated + absorbed) depends only on the relative values of κ, Γ_A and Γ_B. Here, $\Gamma_A = \Gamma^A_{rad} + \Gamma^A_{abs}$, and $\Gamma_B = \Gamma^B_{rad} + \Gamma^B_{abs}$. Hence we first calculate and visualize the dependence of these energies on the relevant parameters κ/Γ_B and Γ_B/Γ_A, in the contour plots shown in Fig. 3.

The way the contour plots are calculated is as follows. For each value of $(\kappa/\Gamma_B, \Gamma_B/\Gamma_A)$ in the adiabatic case, where $\kappa_{12}(t)$ and $\kappa_{23}(t)$ are given by Eqs. (10) and (11), one tries a range of values of t_{EIT}. For each t_{EIT}, the maximum energy transferred $E_3(\%)$ over $0 < t < t_{EIT}$, denoted by $\max(E_3, t_{EIT})$, is calculated together with the total energy lost at that maximum transfer. Next the maximum of $\max(E_3, t_{EIT})$ over all values of t_{EIT} is selected and plotted as a single point on the contour plot in Fig. 3a. We refer to this point as the optimum energy transfer (%) in the EIT-like case for the particular $(\kappa/\Gamma_B, \Gamma_B/\Gamma_A)$ under consideration. We also plot in Fig. 3d the corresponding value of the total energy lost (%) at the optimum of E_3. We repeat these calculations for all pairs $(\kappa/\Gamma_B, \Gamma_B/\Gamma_A)$ shown in the contour plots. In the constant-κ transfer case, for each $(\kappa/\Gamma_B, \Gamma_B/\Gamma_A)$, the time evolution of $E_3(\%)$ and E_{lost} are calculated for $0 < t < 2/\kappa$, and optimum transfer, shown in Fig. 3b, refers to the maximum of $E_3(t)$ over $0 < t < 2/\kappa$. The corresponding total energy lost at optimum constant-κ transfer is shown in Fig. 3e. Now that we calculated the energies of interest as functions of $(\kappa/\Gamma_B, \Gamma_B/\Gamma_A)$, we look for ranges of the relevant parameters in which the EIT-like transfer has advantages over the constant-κ one. So, we plot the ratio of $(E_3)_{EIT-like}/(E_3)_{constant-\kappa}$ in Fig. 3c, and $(E_{lost})_{constant-\kappa}/(E_{lost})_{EIT-like}$ in Fig. 3f. We find that, for $\Gamma_B/\Gamma_A > 50$, the optimum energy transferred in the adiabatic case exceeds that in the constant-κ case, and the improvement factor can be larger than 2. From Fig. 3f, one sees that the EIT-like scheme can reduce the total energy lost by a factor of 3 compared to the constant-κ scheme, also in the range $\Gamma_B/\Gamma_A > 50$.

Although one is usually interested in reducing the total energy lost (radiated + absorbed) as much as possible in order to make the transfer more efficient, the undersirable nature of the radiated energy makes it often important to consider reducing the energy radiated, instead of only considering the total energy lost. For this purpose, we calculate the energy radiated at optimum transfer in both the EIT-like and constant-κ schemes, and compare them. The relevant parameters in this case are κ/Γ_B, Γ_B/Γ_A, Γ^A_{rad}/Γ_A, and Γ^B_{rad}/Γ_B. The problem is more complex because the parameter space is now 4-dimensional. So we focus on those particular cross sections that can best reveal the most important differences between the two schemes. From Fig. 3c and f, one can guess that the best improvement in both E_3 and E_{lost} occurs for $\Gamma_B/\Gamma_A \geqslant 500$. Moreover, knowing that it is the intermediate object R_2 that makes the main difference between the EIT-like and constant-κ schemes, being "energy-empty" in the EIT-like case and "energy-full" in the constant-κ one, we first look at the special situation where $\Gamma^A_{rad} = 0$. In Fig. 4a and b, we show con-

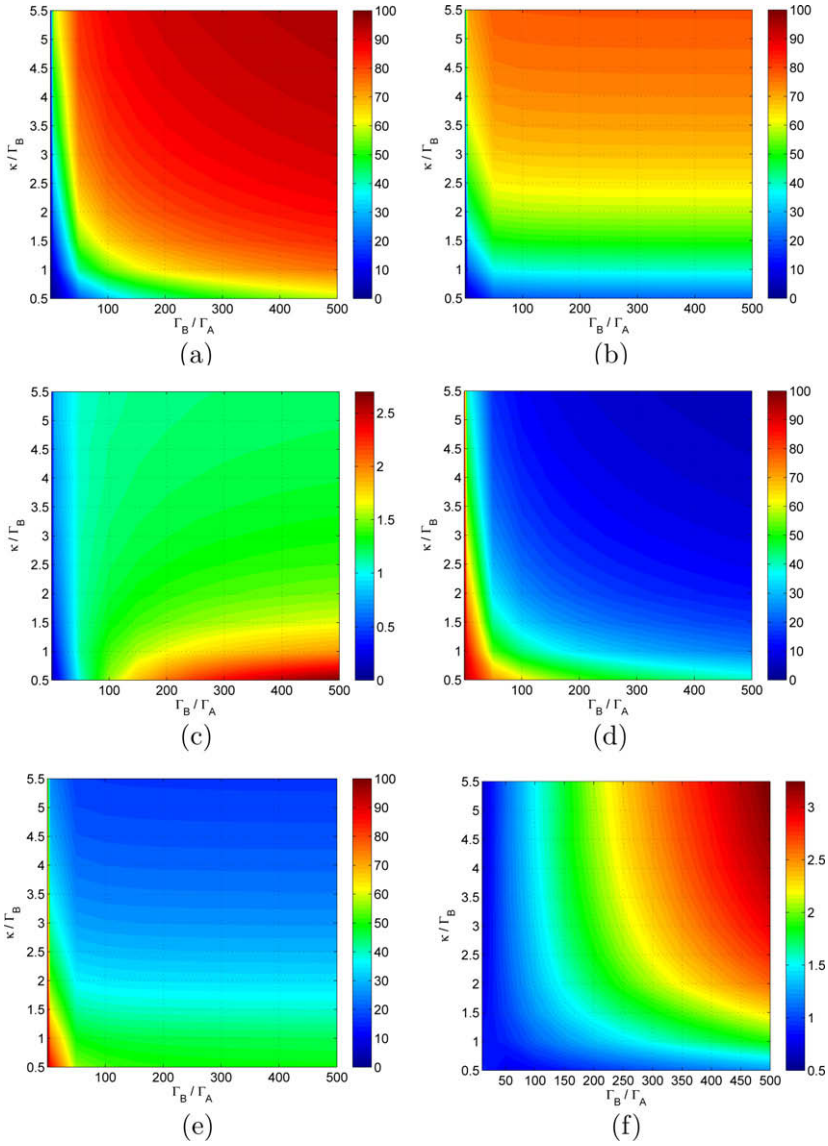

Fig. 3. Comparison between the EIT-like and constant-κ energy transfer schemes, in the general case: (a) Optimum E_3 (%) in EIT-like transfer, (b) optimum E_3 (%) in constant-κ transfer, (c) $(E_3)_{EIT-like}/(E_3)_{constant\text{-}\kappa}$, (d) energy lost (%) at optimum EIT-like transfer, (e) energy lost (%) at optimum constant-κ transfer, (f) $(E_{lost})_{constant\text{-}\kappa}/(E_{lost})_{EIT\text{-}like}$.

tour plots of the energy radiated at optimum transfer, in the constant-κ and EIT-like schemes, respectively, for the particular cross section having $\Gamma_B/\Gamma_A = 500$ and $\Gamma^A_{rad} = 0$. Comparing these two figures, one can see that, by using the EIT-like scheme, one can reduce the energy radiated by a factor of 6.3 or more.

To get a quantitative estimate of the radiation reduction factor in the general case where $\Gamma^A_{rad} \neq 0$, we calculate the ratio of energies radiated at optimum transfers in both schemes, namely,

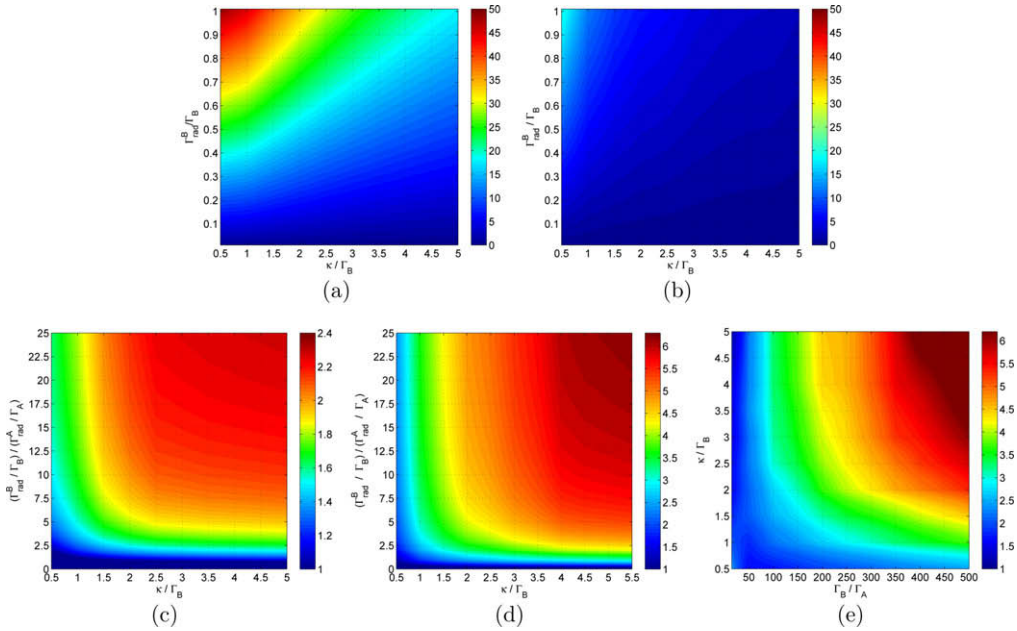

Fig. 4. Comparison between radiated energies in the EIT-like and constant-κ energy transfer schemes: (a) $E_{rad}(\%)$ in the constant-κ scheme for $\Gamma_B/\Gamma_A = 500$ and $\Gamma^A_{rad} = 0$, (b) $E_{rad}(\%)$ in the EIT-like scheme for $\Gamma_B/\Gamma_A = 500$ and $\Gamma^A_{rad} = 0$, (c) $(E_{rad})_{constant\text{-}\kappa}/(E_{rad})_{EIT\text{-}like}$ for $\Gamma_B/\Gamma_A = 50$, (d) $(E_{rad})_{constant\text{-}\kappa}/(E_{rad})_{EIT\text{-}like}$ for $\Gamma_B/\Gamma_A = 500$, (e) $[(E_{rad})_{constant\text{-}\kappa}/(E_{rad})_{EIT-like}]$ as a function of κ/Γ_B and Γ_B/Γ_A, for $\Gamma^A_{rad} = 0$.

$$\frac{(E_{rad})_{constant\text{-}\kappa}}{(E_{rad})_{EIT\text{-}like}} = \frac{\int_0^{t_{opt}^{constant\text{-}\kappa}} \left\{ \frac{\Gamma^B_{rad}}{\Gamma^A_{rad}} |a_2^{constant\text{-}\kappa}(t)|^2 + \left(|a_1^{constant\text{-}\kappa}(t)|^2 + |a_3^{constant\text{-}\kappa}(t)|^2 \right) \right\} dt}{\int_0^{t_{opt}^{EIT\text{-}like}} \left\{ \frac{\Gamma^B_{rad}}{\Gamma^A_{rad}} |a_2^{EIT\text{-}like}(t)|^2 + \left(|a^{EIT\text{-}like}(t)|^2 + |a_3^{EIT\text{-}like}(t)|^2 \right) \right\} dt} \tag{15}$$

which depends only on $\Gamma^B_{rad}/\Gamma^A_{rad}$, the time-dependent mode amplitudes, and the optimum transfer times in both schemes. The latter two quantities are completely determined by κ/Γ_B, and Γ_B/Γ_A. Hence the only parameters relevant to the calculations of the ratio of radiated energies are $\Gamma^B_{rad}/\Gamma^A_{rad}$, κ/Γ_B, and Γ_B/Γ_A, thus reducing the dimensionality of the investigated parameter space from 4 down to 3. For convenience, we multiply the first relevant parameter $\Gamma^B_{rad}/\Gamma^A_{rad}$ by Γ_A/Γ_B, which becomes $(\Gamma^B_{rad}/\Gamma_B)/(\Gamma^A_{rad}/\Gamma_A)$, i.e. the ratio of quantities that specify what percentage of each object's loss is radiated. Next, we calculate the ratio of energies radiated as a function of $(\Gamma^B_{rad}/\Gamma_B)/(\Gamma^A_{rad}/\Gamma_A)$ and κ/Γ_B, in the two special cases $\Gamma_B/\Gamma_A = 50$, and $\Gamma_B/\Gamma_A = 500$, and we plot them in Fig. 4c and d, respectively. We also show, in Fig. 4e, the dependence of $(E_{rad})_{constant\text{-}\kappa}/(E_{rad})_{EIT\text{-}like}$ on κ/Γ_B and Γ_B/Γ_A, for the special case $\Gamma^A_{rad} = 0$. As can be seen from Fig. 4c and d, the EIT-like scheme is less radiative than the constant-κ scheme whenever $(\Gamma^B_{rad}/\Gamma_B)$ is larger than $(\Gamma^A_{rad}/\Gamma_A)$, and the radiation reduction ratio increases as Γ_B/Γ_A and κ/Γ_B are increased (see Fig. 4e).

5. Conclusion

In conclusion, we proposed an efficient weakly radiative energy transfer scheme between two identical resonant objects, based on an EIT-like transfer of the energy through a mediating resonant object with the same resonant frequency. We analyzed the problem using CMT, and pointed out that the fundamental principle underlying our energy transfer scheme is similar to the known EIT process [9] in which there is complete population transfer between two quantum states. We also explored

how the EIT-like scheme compares to the constant-κ one, as the relevant parameters of the system are varied. We motivated all this, initially, by specializing to the problem of witricity-like wireless energy transfer between inductively-coupled metallic loops. However, our proposed scheme, not being restricted to the special type of resonant inductive coupling, is not bound only to wireless energy transfer, and could potentially find applications in various other unexplored types of coupling between general resonant objects. In fact, in this context, the work presented here generalizes the concept of EIT, previously known as a quantum mechanical phenomenon that exists in microscopic systems, to a more general energy transfer phenomenon, between arbitrary classical resonant objects. We focused on the particular example of electromagnetic resonators, but the nature of the resonators and their coupling mechanisms could as well be quite different, e.g. acoustic, mechanical, etc. Since all these resonant phenomena could be modeled with nearly identical CMT equations, the same behavior would occur.

Acknowledgments

Finally, we acknowledge Dr. Peter Bermel and Prof. Steven G. Johnson for their help. This work was supported in part by the Materials Research Science and Engineering Center Program of the National Science Foundation under award DMR 02-13282, the Army Research Office through the Institute for Soldier Nanotechnologies contract W911NF-07-D-0004, DARPA via the U.S. Army Research Office under contract W911NF-07-D-0004, the U.S. Department of Energy under award number DE-FG02-99ER45778, and by a grant from 3M. We also acknowledge support of the Buchsbaum award.

Appendix A

A.1. Analytical solution of the 3-object system in the constant-κ case

The CMT equations Eq. (12) admit a simple analytical solution in the special case where the coupling rates $\kappa_{12}(t)$ and $\kappa_{23}(t)$ are independent of time and equal to each other, namely when $\kappa_{12} = \kappa_{23} =$ constant independent of time. After making the following set of substitutions

$$\Sigma \equiv \frac{1}{U} \equiv \frac{\Gamma_A + \Gamma_B}{2\sqrt{2}\kappa} \tag{16}$$

$$\Delta \equiv \frac{\Gamma_B - \Gamma_A}{2\sqrt{2}\kappa} \tag{17}$$

$$T \equiv \sqrt{2}\kappa t \tag{18}$$

we obtain the expressions below for the time-varying amplitudes

$$a_1(T) = \frac{1}{2} e^{-i\omega t} e^{-\Sigma T} \left[\frac{\Delta}{\sqrt{\Delta^2 - 1}} sinh\left(\sqrt{\Delta^2 - 1}T\right) + cosh\left(\sqrt{\Delta^2 - 1}T\right) + e^{-\Delta T} \right] \tag{19}$$

$$a_2(T) = i e^{-i\omega t} e^{-\Sigma T} \frac{1}{\sqrt{\Delta^2 - 1}} sinh\left(\sqrt{\Delta^2 - 1}T\right) \tag{20}$$

$$a_3(T) = \frac{1}{2} e^{-i\omega t} e^{-\Sigma T} \left[\frac{\Delta}{\sqrt{\Delta^2 - 1}} sinh\left(\sqrt{\Delta^2 - 1}T\right) + cosh\left(\sqrt{\Delta^2 - 1}T\right) - e^{-\Delta T} \right] \tag{21}$$

The time t_{opt} at which the energy transferred to R_3 is optimum, can be obtained by setting the time derivative of the energy $|a_3(T)|^2$ in R_3 to zero, and is therefore a solution to the following equation

$$\Sigma \left[\frac{\Delta}{\sqrt{\Delta^2 - 1}} sinh\left(\sqrt{\Delta^2 - 1}T\right) + cosh\left(\sqrt{\Delta^2 - 1}T\right) \right] -$$
$$\Delta \left[\frac{\sqrt{\Delta^2 - 1}}{\Delta} sinh\left(\sqrt{\Delta^2 - 1}T\right) + cosh\left(\sqrt{\Delta^2 - 1}T\right) \right] = (\Sigma - \Delta) e^{\Delta T} \tag{22}$$

In general, this equation may not have an obvious analytical solution, but it does admit a simple solution in the two special cases that we will consider below.

In the first special case, we set $\Delta = 0$, and thus we have $\Gamma_A = \Gamma_B = \Gamma$ and $\Sigma = \frac{1}{U} = \frac{\Gamma}{\sqrt{2}\kappa}$. In this case, $T_{opt} \equiv \sqrt{2}\kappa t_{opt}$ becomes

$$T_{opt} = 2\ tan^{-1}\left(\frac{1}{\Sigma}\right) = 2\ tan^{-1}U \tag{23}$$

and the efficiency of the 3-object system becomes

$$\eta \equiv \frac{|a_3(T_{opt})|^2}{|a_1(0)|^2} = \left[\frac{U^2}{1+U^2}exp\left(\frac{-2tan^{-1}U}{U}\right)\right]^2 \tag{24}$$

which is just the square of the efficiency of the two-object system [6]. Therefore, when all objects are the same, the efficiency of the 3-object system at optimum is equal to the square of the efficiency of the 2-object system, and hence is smaller than it.

In the second special case, we set $\Delta = \Sigma = \frac{1}{U} = \frac{\Gamma_B}{2\sqrt{2}\kappa}$, that is to say we set $\Gamma_A = 0$. The analytical expressions for T_{opt} and η become, respectively

$$T_{opt} = \begin{cases} \frac{\pi U}{\sqrt{U^2-1}},\ U > 1 \\ \infty,\ U \leqslant 1 \end{cases} \tag{25}$$

$$\eta = \begin{cases} \frac{1}{4}\left[1 + \exp\left(\frac{-\pi}{\sqrt{U^2-1}}\right)\right]^2,\ U > 1 \\ \frac{1}{4},\ U \leqslant 1 \end{cases} \tag{26}$$

Therefore, the optimum efficiency in this case, is larger when $\kappa > \frac{\Gamma_B}{2\sqrt{2}}$.

A.2. Resolution of apparent paradox in EIT-like scheme

As we said earlier in the text, the explanation of the EIT-like scheme in terms of the adiabatic following of the eigenstate $\vec{V}_1$, seems to be puzzling and somewhat paradoxical. The reason is that energy is efficiently transferred through the intermediate resonator R_2 without ever being in it. This apparent contradiction can be resolved by looking at the detailed contributions to the time-rate of change of the energy E_2 in R_2. Since the energy in R_2 at time t is $E_2(t) = |a_2(t)|^2$, one can use the CMT Eq. (12) and calculate the power $dE_2(t)/dt$ through R_2, to obtain

$$\frac{d|a_2|^2}{dt} = -2\Gamma_B|a_2|^2 - 2\kappa_{12}\mathrm{Im}(a_2^* a_1) + 2\kappa_{23}\mathrm{Im}(a_3^* a_2). \tag{27}$$

The first term on the right-hand side of this equation corresponds to the total power lost in R_2. The second term can be identified with the time-rate $P_{12}(t)$ of energy transfer from R_1 to R_2, namely $P_{12}(t) = -2\kappa_{12}(t)\mathrm{Im}(a_2^*(t)a_1(t))$. Similarly, the third term can be identified with the time-rate $P_{23}(t)$ of energy transfer from R_2 to R_3: $P_{23}(t) = 2\kappa_{23}(t)\mathrm{Im}(a_3^*(t)a_2(t))$. Note that because $P_{12}(t)$ represents the rate at which energy gets into R_2 (coming from R_1), this term will be positive. Similarly, because $P_{23}(t)$ is the rate at which energy gets out of R_2 (going to R_3), this term will be negative. For simplicity, we will focus on the case where $\Gamma_A = \Gamma_B = 0$, and take the time variation of the coupling rates to be given by Eqs. (10) and (11). In this case, the total energy in the 3-object system is conserved, and the change in the energy E_2 can arise only from the exchange of energy between R_1 and R_2, and between R_2 and R_3. In this special case, the rate of change of E_2, which equals the sum $P_{12} + P_{23}$, is oscillatory in time with amplitude A_{sum}. It turns out that as the transfer time t_{EIT} gets longer, the peak amplitude A_{sum} of the sum $P_{12} + P_{23}$ approaches zero. This means that at the moment when energy reaches R_2 from R_1, it leaves R_2 immediately to R_3. Therefore, $dE_2(t)/dt$ is almost zero $\forall\ t$, and the energy in R_2 remains approximately equal to its initial value of zero throughout the EIT-like transfer, despite the fact that all the energy initially in R_1 goes through R_2 as it gets transferred to R_3. To illustrate this point, we consider again the case $\Gamma_A = \Gamma_B = 0$, and choose the coupling rate κ such that $Q_\kappa = 1000$. In Fig. 5a, we plot the powers P_{12}, P_{23} and their sum as functions of time when the duration of the transfer is

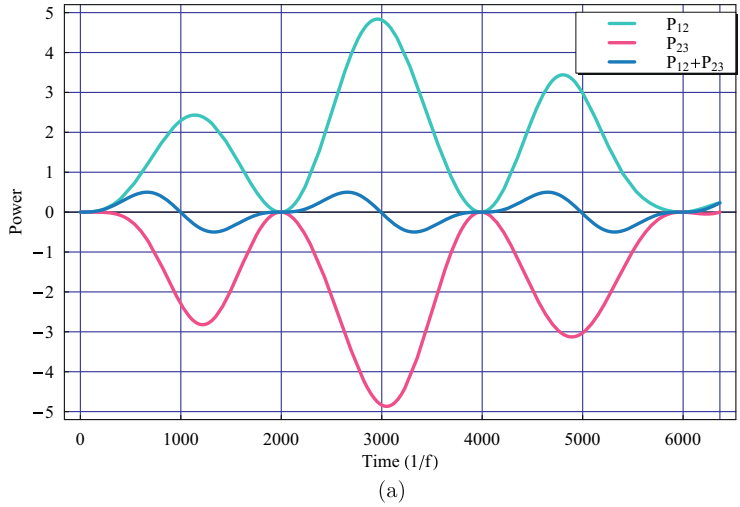

(a)

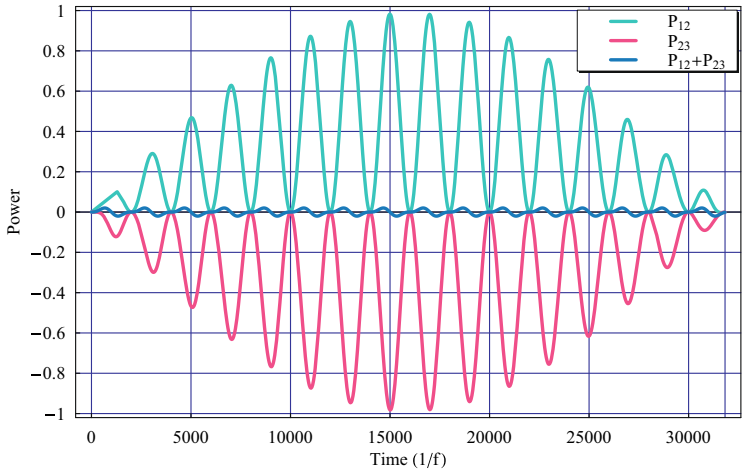

(b)

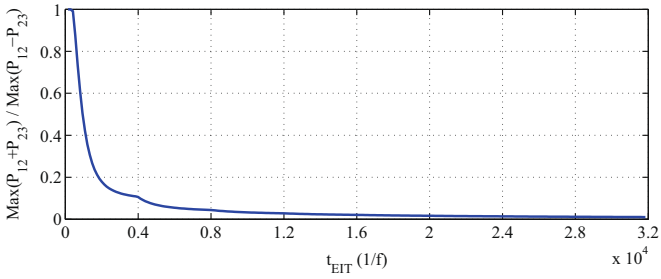

(c)

Fig. 5. (a) P_{12}, P_{23} and $P_{12}+P_{23}$ as functions of time for $\Gamma_A = \Gamma_B = 0$, $Q_\kappa = 1000$, and $t_{EIT} = 6366.2(1/f)$. (b) Same plot as in (a) but with t_{EIT} five times longer. (c) $\mathrm{Max}(P_{12}+P_{23})/\mathrm{max}(P_{12}-P_{23})$ versus t_{EIT} for $\Gamma_A = \Gamma_B = 0$ and $Q_\kappa = 1000$.

$t_{EIT} = 6366.2(1/f)$. In Fig. 5b, we repeat the same plots but now with a transfer time five times longer. As can be seen by comparing Fig. 5a and b, we find that the relative amplitude A_{sum}, compared to characteristic magnitudes of P_{12} and P_{23}, has dramatically decreased. To get a quantitative estimate of this decrease in the amplitude of $P_{12} + P_{23}$, we show in Fig. 5c, the ratio of A_{sum} over the maximum of $P_{12} - P_{23}$ as a function of t_{EIT}. We find that, indeed, as the transfer time gets longer, meaning that the adiabatic condition is better satisfied, the amplitude A_{sum} gets smaller and smaller compared to the peak of P_{12}, and consequently the deviation of the energy in R_2 from its initial zero value becomes negligible. Therefore, one way to look at why the EIT mechanism works so well, is to note that the EIT-approach ensures that the energy leaves R_2 (to R_3) as soon as it reaches R_2 (from R_1).

References

[1] J.M. Fernandez, J.A. Borras, Contactless battery charger with wireless control link, US patent number 6,184,651 issued in February 2001.
[2] L. Ka-Lai, J.W. Hay, P.G.W. Beart, Contact-less power transfer, US patent number 7,042,196 issued in May 2006 (SplashPower Ltd., <www.splashpower.com>).
[3] A. Esser, H.-C. Skudenly, IEEE Trans. Industry Appl. 27 (1991) 872.
[4] J. Hirai, T.-W. Kim, A. Kawamura, IEEE Trans. Power Electron. 15 (2000) 21.
[5] G. Scheible, B. Smailus, M. Klaus, K. Garrels, L. Heinemann, System for wirelessly supplying a large number of actuators of a machine with electrical power, US patent number 6,597,076, issued in July 2003 (ABB, <www.abb.com>).
[6] Aristeidis Karalis, John D. Joannopoulos, Marin Soljacic, Ann. Phys. 323 (2008) 34.
[7] Andre Kurs, Aristeidis Karalis, Robert Moffatt, J.D. Joannopoulos, Peter Fisher, Marin Soljacic, Science 317 (2007) 83.
[8] Stephen E. Harris, Phys. Today 50 (7) (1997) 36–42.
[9] K. Bergmann, H. Theuer, B.W. Shore, Rev. Mod. Phys. 70 (3) (1998) 1003–1023.
[10] J.R. Kuklinski, U. Gaubatz, F.T. Hioe, K. Bergmann, Phys. Rev. A 40 (1989) 6741–6744.
[11] U. Gaubatz, P. Rudecki, S. Schiemann, K. Bergmann, J. Chem. Phys. 92 (1990) 5363.
[12] H.A. Haus, Waves and Fields in Optoelectronics, Prentice-Hall, NJ, 1984.